



Vitrification of high chrome oxide nuclear waste in iron phosphate glasses

Wenhai Huang^{a,*}, Delbert E. Day^b, Chandra S. Ray^b,
Cheol-Woon Kim^b, Andrea Mogus-Milankovic^c

^a School of Materials Science and Engineering, Tongji University, Shanghai 200092, PR China

^b Graduate Center for Materials Research and Department of Ceramic Engineering, University of Missouri-Rolla,
Rolla, MO 65409-1170, USA

^c Department of Physics, Ruder Bokovic Institute, 10000, Zagreb, Croatia

Received 3 September 2003; accepted 29 January 2004

Abstract

A simulated high level waste (HLW) containing 4 mass% chrome oxide, whose overall composition is representative of the high chrome oxide wastes at Hanford WA USA, was easily vitrified in a phosphate glass at temperatures ranging from 1150 °C, for waste loadings of 55 mass%, to 1250 °C for waste loadings of 75 mass%. Even at these high waste loadings, these wasteforms had an excellent chemical durability. The best chemical durability was achieved when the O/(Si + P) atomic ratio was between 3.5 and 3.8. These wasteforms were also resistant to crystallization although trace amounts of crystalline Cr₂O₃ were present in wasteforms containing more than 70 mass% HLW. It is concluded that up to 45 mass% of the total HLW at Hanford, especially that containing as high as 4.5 mass% chrome oxide, could be directly vitrified into an iron phosphate glass, that meets all of the current chemical durability requirements by simply adding 25–35 mass% P₂O₅ to the waste and melting the mixture at 1150–1250 °C for a few (<6) hours.

© 2004 Elsevier B.V. All rights reserved.

PACS: 81.05.P; 61.43.F; 81.70; 82.80

1. Introduction

There is an estimated that 12.3×10^6 kg of high level nuclear waste (HLW) stored in 177 underground tanks at Hanford, WA, USA [1] which will be treated for permanent disposal. This HLW has been divided into 17 compositional groups (called clusters) which contain varying amounts of chrome oxide, 4.5 mass% Cr₂O₃ being the highest. Cr₂O₃ is a refractory oxide, melting point of 2330 °C, that is only slightly soluble in most silicate-type melts. Because of its low solubility, Cr₂O₃ is

often a component of the refractory used to contain high temperature silicate and borosilicate melts.

The chemical solubility of Cr₂O₃ in alkali aluminium borosilicate (AABS) glass is about 0.5 mass% [2]. To vitrify the HLW containing 4.5 mass% Cr₂O₃ needs nine times of HLW volume of AABS glass. The cost for treating this HLW would increase tremendously. Many efforts have been made for increasing the solubility of Cr₂O₃ in AABS glass, but the highest solubility of Cr₂O₃ is still only 1 mass% [3]. Therefore AABS glass is not the best accommodation glass for the HLW at Hanford. An iron phosphate glass might be a suitable alternative to immobilize this HLW, since it could dissolve Cr₂O₃ more easily.

The HLW at Hanford also contains oxides, such as P₂O₅, Fe₂O₃, Bi₂O₃, rare earth oxides like La₂O₃, and heavy metal oxides like U₃O₈, which are also difficult to

* Corresponding author. Address: Graduate Center for Materials Research and Department of Ceramic Engineering, University of Missouri-Rolla, Rolla, MO 65409-1170, USA.

E-mail address: whhuang@mail.tongji.edu.cn (W. Huang).

be dissolved uniformly in AABS glasses, but which are more soluble in phosphate glasses [4,5]. Because of the inherently higher solubility of these oxides in phosphate glasses, chemically durable iron phosphate glasses could potentially reduce the volume of the final wasteform.

A major objective of the present study was to investigate the vitrification of the high chrome wastes at Hanford in iron phosphate glasses. Another objective was to determine the maximum waste loading and the chemical durability of the wasteforms containing high chrome by different methods. The chemical durability of both glassy and deliberately crystallized wasteforms was determined from dissolution rate (DR), vapor hydration test (VHT) and product consistency test (PCT) measurements.

To simulate the cooling experiences in a metal canister, selected iron phosphate melts were cooled from their melting temperature to their crystallization temperature (870 °C) at 2 °C min⁻¹, held at 870 °C for 2 h,

cooled to 300 °C at 2 °C min⁻¹ and slowly thereafter cooled to room temperature. The chemical durability of these wasteforms was measured and is reported herein.

2. Experimental procedure

2.1. Simulated waste composition

The HLW at Hanford [1] has been divided into 17 compositional clusters, which contain from 0.11 to 4.25 mass% Cr₂O₃ and whose combined mass is estimated to be 12.3 × 10⁶ kg. The composition of the waste in clusters #7, 8 and 14, which are the three highest Cr₂O₃-containing wastes at Hanford, is given in Table 1, along with the estimated amount of each waste (bottom line). Rather than investigate each waste separately, it was decided to use a simplified waste composition that was a blend of the waste in clusters #7, 8, and 14. The

Table 1

Nominal composition, mass%, of the high chrome nuclear waste for clusters #7, 8 and 14 at Hanford, WA., the total mass (Mg) of waste in each cluster, and the composition, mass%, of the simulated 'simplified blend' waste (right hand column) used in the present work

Component	Cluster ^a			Blend %	Combined blend	Simplified blend (%)	
	#7	#8	#14				
Al ₂ O ₃	18.07	23.03	14.97	19.60	+(B ₂ O ₃)	20.47	21
As ₂ O ₅	0.03	1.30	0.54	0.57	–		
B ₂ O ₃	0.27	1.96	0.76	0.87			
Bi ₂ O ₃	0.39	2.11	1.58	1.18	+(PbO,Tl ₂ O)	2.41	3
CaO	1.97	1.45	0.78	1.64	+(MgO,SrO)	2.82	(CaF ₂) 3
CdO	0.01	0.03	0.10	0.03	–		
Ce ₂ O ₃	0.04	1.02	0.45	0.46			
Cr ₂ O ₃	2.02	2.51	4.25	2.46	+(MnO)	3.84	4
F	1.04	1.21	1.39	1.15		1.15	
Fe ₂ O ₃	8.38	7.25	10.96	8.25	+(NiO)	8.75	9
K ₂ O	0.77	0.16	1.97	0.67			
La ₂ O ₃	0.06	0.06	0.21	0.07	+(Ce ₂ O ₃ , Nd ₂ O ₃)	0.97	1
MgO	0.06	2.33	0.65	0.98			
MnO	1.04	1.83	1.40	1.38			
Na ₂ O	21.08	27.20	35.50	25.03	+(K ₂ O)	25.70	26
Nd ₂ O ₃	0.02	0.99	0.42	0.44			
NiO	0.43	0.59	0.55	0.50			
P ₂ O ₅	2.10	6.40	2.44	3.78		3.87	5
PbO	0.50	0.44	0.52	0.48			
SiO ₂	27.5	4.39	2.02	15.87		15.87	16
SrO	0.14	0.32	0.09	0.20			
ThO ₂	0.36	0.25	0.20	0.29			
Tl ₂ O	0.04	1.71	0.74	0.75			
U ₃ O ₈	10.66	6.87	5.15	8.60	+(ThO ₂)	8.89	9
ZrO ₂	2.24	0.70	10.23	2.57		2.57	3
Total	99.24	96.10	97.88	97.89		97.29	100
Others	0.76	3.90	2.12	2.11		2.71	
Mass (10 ⁶ g)	678	506	150	1334			

^a Chemical composition is from Ref. [1].

composition, in the column labeled 'Blend' in Table 1, was calculated for each oxide according to Eq. (1):

$$m_x = \left[\frac{\sum (M_i \cdot m_{xi})}{1334} \right], \quad (1)$$

where m_x is the mass% of 'oxide X' in the Blend (fifth column from left, Table 1), M_i is the total mass of cluster ' i ', m_{xi} is the mass% of 'oxide X' in cluster ' i ', $i = 7, 8$ and 14 , and 1334 is the combined mass (10^6 g) of all three clusters.

The number of individual (oxide) components in the waste was reduced by combining different oxides that play a similar role in a glass, as shown in the column labeled 'combined blend' in Table 1, and ignoring those components whose amount was below 0.5%. For example, Na_2O and K_2O behave similarly in a glass, so the Na_2O (25.03%) and K_2O (0.67%) in the Blend column were added together (25.70%). This sum was then used as the mass fraction for the major component, in this case Na_2O , in the combined blend. The composition of the 'combined blend' was further simplified by rounding to the nearest whole percent, see right hand column ('simplified blend') in Table 1. It is to be noted that CaF_2 , instead of CaO , was used in the simplified blend to provide the fluorine present in the three wastes. The overall composition of the 'simplified waste' (right hand column in Table 1), contains 4 mass% Cr_2O_3 , which is just slightly less than the maximum Cr_2O_3 content (4.25 mass%) of the waste in cluster #14 at Hanford.

2.2. Glass melting

Batches that produced 50–100 g of glass of the general mass% composition $x(W) \cdot (100 - x)\text{P}_2\text{O}_5$ were prepared by mixing the appropriate amounts of the oxides listed in the right hand column of Table 2. W denotes the simplified waste and x ranged from 35 to 90

in 5% intervals. Note that the P_2O_5 required was added arbitrarily as sodium phosphate. To compensate for the volatilization of P_2O_5 , an additional 5 mass% of the required amount of P_2O_5 was added to the batch.

Each batch was ground to minus 100 mesh, dry mixed by tumbling in a sealed plastic container, and then melted in a alumino-silicate crucible between 1100 (waste content 35%) and 1300 °C (waste content >80%) for 2 h in air. Each melt was stirred two times at 30 min intervals with a silica glass rod to aid homogenization. The melts were cast into a steel mold to form rectangular bars $\sim 1 \text{ cm} \times 1 \text{ cm} \times 5 \text{ cm}$. The bars were annealed between 520 and 540 °C for 4 h and slowly cooled (overnight) in the annealing furnace to room temperature. Corrosion of the crucible by these iron phosphate melts was barely detectable.

Each glass was identified as 'IP(x)W', where 'IP' stands for iron phosphate and ' x ' is the mass% of simulated waste (W), or waste loading in the glass. Thus, a designation as IP70W means an iron phosphate glass with a simulated waste (W) loading of 70 mass%. The batch composition for two noteworthy glasses, IP70W and IP75W, is given in Table 2 along with the raw materials used in the batch. CaF_2 in the batch is considered to have converted to CaO and dissolved fluorine during melting. Note the relatively high soda content of these glasses is close to 20 mass%. Powder X-ray diffraction (XRD) was used to determine the amorphous or crystalline character of the annealed samples.

2.3. Heat treatment

2.3.1. Melt cooled in furnace

As mentioned previously, the IP70W melt was cooled in the electric melting furnace at $2 \text{ }^\circ\text{C min}^{-1}$ from its melting temperature of 1250 °C to its crystallization temperature of 870 °C where it was held for 2 h. It was then cooled to 300 °C at $2 \text{ }^\circ\text{C min}^{-1}$ and then slowly

Table 2

Composition, mass%, of simulated waste, and iron phosphate wastefoms containing 70 mass% (IP70WG) and 75 mass% (IP75WG) of the simulated waste; chemicals used in the batch are shown

Component	Simulated waste	IP70WG	IP75WG	Chemicals used
AlF_2O_3	21	14.70	15.75	$\text{Al}(\text{OH})_3$
Bi_2O_3	3	2.10	2.25	Bi_2O_3
CaF_2^a	3	2.10	2.25	CaF_2^a
Cr_2O_3	4	2.80	3.00	Na_2CrO_4
Fe_2O_3	9	6.30	6.75	Fe_2O_3
La_2O_3	1	0.70	0.75	La_2O_3
Na_2O	26	18.20	19.50	Na_2CO_3
P_2O_5	5	33.50	28.75	$\text{NaH}_2\text{PO}_4 \cdot 2\text{H}_2\text{O}$
SiO_2	16	11.20	12.00	$\text{Na}_2\text{SiO}_3 \cdot 5\text{H}_2\text{O}$
U_3O_8	9	6.30	6.75	UO_2
ZrO_2	3	2.10	2.25	ZrO_2

^a CaF_2 in batch converted to CaO and dissolved fluorine during melting.

cooled to room temperature. The crucible was deliberately broken in order to remove the slowly cooled samples that were used for the dissolution rate (DR) measurements.

2.3.2. Crystallized samples

There were no distinct crystallization peaks observed in the DTA curves of the IP65W, IP70W, IP75W and IP80W annealed samples, up to their melting temperature, but a small inflection ~ 100 °C higher than the transition temperature was attributed to crystallization. Therefore, these glasses were heat treated (i.e., deliberately crystallized) at 650 °C for 48 h in air. These crystallized samples were used for DR, PCT and VHT measurements.

2.4. X-Ray diffraction (XRD)

2.4.1. Qualitative analysis

All the annealed samples were crushed into <45 μm particles and examined by XRD to check for crystalline phases. The XRD results in Table 3 indicated that all these samples were glassy, except for IP70W, IP75W and IP80W, which contained a barely detectable amount <1.5 mass%, of crystalline Cr_2O_3 (see Fig. 1). Melts IP85W and IP90W were too viscous to pour at 1300 °C and are not listed in Table 3 since these melts crystallized during cooling.

2.4.2. Determination of crystalline Cr_2O_3 content

Fig. 1 shows that the intensity of the barely detectable diffraction peaks for crystalline Cr_2O_3 increased slightly with increasing waste loading from IP70W to IP80W. To measure how much crystalline Cr_2O_3 was present, XRD standards were made using a mixture of crystalline Cr_2O_3 and the IP65W glass whose XRD pattern is close to the background for the other samples. A calibration curve for the standards was determined using the equation:

$$\frac{I_A}{I_G} = K \cdot C_A, \quad (2)$$

where I_A is the net intensity (total intensity minus the background) of the diffraction peak for crystalline Cr_2O_3 , I_G is the background intensity at the peak, K is a constant and C_A is the weight fraction of crystalline Cr_2O_3 in the standard. In the present study, the background intensity for the glassy IP65W sample was more constant from 10° to 30° than from 30° to 38° . Therefore the XRD peak at 24.5° was chosen rather than the slightly larger peak at 33.6° . The concentration of crystalline Cr_2O_3 in the standards, C_A was 1, 3, 5, 7 and 10 mass%.

The ratio I_A/I_G for the peak at 24.5° is plotted in Fig. 2 as a function of C_A . Using this calibration curve, the

Table 3
Melting temperature and time and selected properties of high chrome iron phosphate wasteforms (after normal annealing)

Waste form ID	IP35W	IP40W	IP45W	IP50W	IP55W	IP60W	IP65W	IP70W	IP75W	IP80W
Tm (°C)	1100	1100	1100	1150	1150	1200	1200	1250	1250	1300
Hm (h)	2	2	2	2	2	2	2	2	2	2
XRD check	Glass	Glass	Glass	Glass	Glass	Glass	Glass	Glass ^a	Glass ^a	Glass ^a
Color	G	G	G	G	G	G	B	B	B	DB
Density ^b (g cm ⁻³)	2.69	2.71	2.75	2.77	2.84	2.84	2.86	2.89	2.92	2.97

Tm: melting temperature; Hm: melting time; G: green; B: black; DB: dark brown.

^a Glass contained <1.5 mass% crystalline Cr_2O_3 .

^b Estimated error is $\pm 0.4\%$.

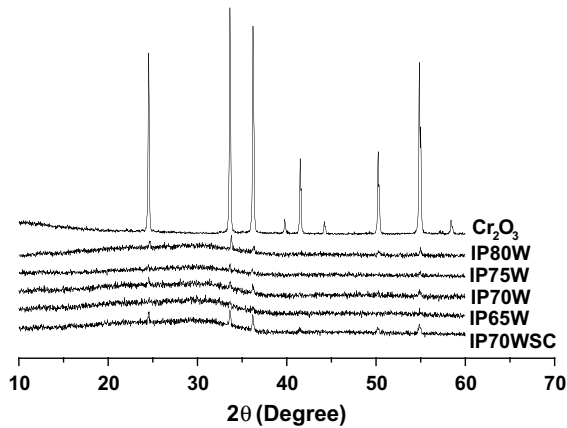


Fig. 1. XRD pattern for Cr_2O_3 containing iron phosphate wasteforms, annealed. Trace amounts of crystalline Cr_2O_3 are evident in the samples with ≥ 70 mass% waste loading. The curve IP70WSC is for a sample cooled at $2^\circ\text{C}/\text{min}$ from its melting temperature, with a 2 h hold at 870°C .

concentration of crystalline Cr_2O_3 in the IP70W, IP75W and IP80W samples was calculated and is shown by the open circles in Fig. 3. The total amount of Cr_2O_3 (filled circles) in the starting batch from the sodium chromate is shown for comparison.

2.5. Chemical durability measurements

The chemical durability of each wasteform was measured in three ways: (1) dissolution rate (DR) [6], calculated from the weight loss of bulk samples immersed in deionized water (DIW) at 90°C for up to 128 days; (2) vapor hydration test (VHT) [7] (200°C for 7 days); and (3) product consistency test (PCT) [8], mea-

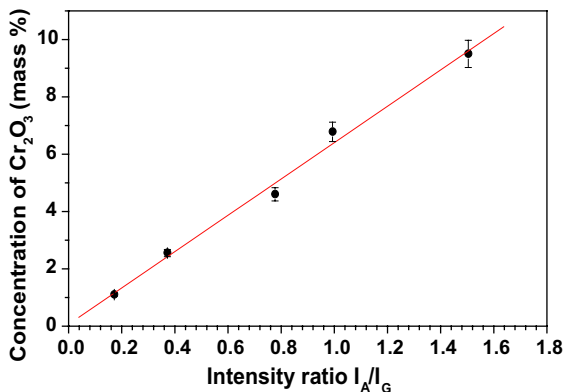


Fig. 2. Calibration curve derived from the relationship of intensity ratio of XRD peak at 24.5° for crystalline Cr_2O_3 (see Fig. 1) with the concentration of crystalline Cr_2O_3 in the standards, consisting of powdered IP65W glass mixed with varying amounts of crystalline Cr_2O_3 .

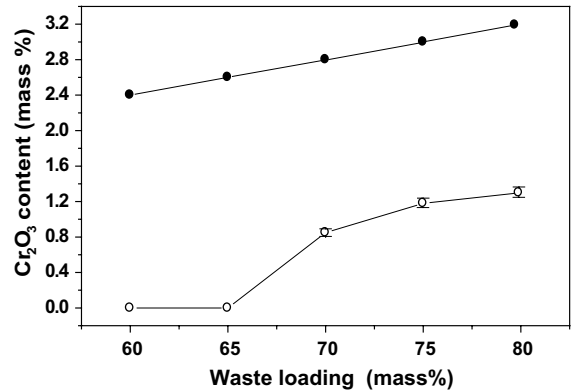


Fig. 3. Weight percent Cr_2O_3 in the starting batch (dark circles) and percent crystalline Cr_2O_3 detected by XRD in the annealed glass (open circles), as calculated from the calibration curve in Fig. 2. Estimated error is represented by size of data points.

sured from the amount of ions released from powders immersed in DIW at 90°C for 7 days (ASTM C-1285-97). The VHT and PCT were measured for both glassy and crystallized samples of IP70W and IP75W.

2.5.1. Dissolution rate (DR)

Specimens were cut into $1 \times 1 \times 1$ cm cubes from annealed glassy bars or crystallized bars. The surfaces were ground progressively using 240, 600 and 800-grit SiC paper with oil as the cooling agent. For the IP70W-SC sample that was cooled in the furnace and removed from the crushed crucible, the pieces were too small to be cut into a 1 cm cube so an irregular shaped sample was used. Each bulk sample was rinsed with acetone and DIW, dried at 90°C for 30 min and cooled to room temperature. This rinsing procedure was followed before each weighing during the corrosion test. The exact size (± 0.01 cm) and weight (± 0.01 mg) of each specimen was measured.

Each sample was suspended by a thin rayon thread and immersed in 100 ml of DIW in a plastic bottle. The plastic bottle was placed in a 90°C oven. The sample was removed after 128 days, rinsed with DIW to remove precipitation of secondary layers on the surface, dried at 90°C , cooled and weighed (± 0.01 mg). The weight loss of the sample and the pH of the leachate were measured.

The DR of each sample was calculated from the equation:

$$\text{DR} = \frac{\Delta W}{At}, \quad (3)$$

where ΔW is the measured weight loss in gram; A is the sample surface area in cm^2 , and t is the immersion time in minute.

Duplicate samples were measured and the error in the average value reported herein is $\pm 15\%$.

2.5.2. Vapor hydration test (VHT)

The VHT was performed on $10 \times 10 \times 1.5$ mm (the surface area 251–268 mm²) samples, both annealed glassy and crystallized. After the surface of each sample was polished with 600-grit SiC paper, its weight (± 0.01 mg) and size were measured (the thickness was measured with optical microscope). Each sample was washed with flowing DIW, ultrasonically cleaned in ethanol and dried at 90 °C. Duplicate IP70W and IP75W samples, both glassy and crystallized, were suspended from a support rod with a thin Teflon thread in separate stainless steel vessels containing 0.25 ml DIW. The vessels were placed in an oven at 200 °C for 7 days.

After completion of VHT, the samples were removed from the vessel, and cross-sectioned with a diamond saw. The polished cross-section of each sample was examined with an optical microscope and the thickness of the un-corroded sample was measured. The amount of corroded sample, m_d (g/m²) was calculated from the difference between the initial thickness of the sample, d_i and the thickness of the remaining (un-corroded) layer, d_f , the initial size, w_i , l_i , d_i and weight, m_i , and the final size w_f , l_f , d_f , and weight m_f , of the sample using the equation:

$$m_d = \frac{\Delta m}{S} = \frac{m_i - m_f}{2(w_i l_i + l_i d_i + d_i w_i)} \approx \frac{\rho w_i l_i d_i - \rho w_f l_f d_f}{2w_i l_i} = \frac{\rho(d_i - d_f)}{2}, \quad (4)$$

where Δm is the weight loss (or gain) and ρ is the sample density. The error in m_d calculated from Eq. (4) is estimated at $\pm 5\%$.

2.5.3. Product consistency test (PCT)

The PCT was conducted on duplicate powder samples per the procedures in ASTM C-1285-97. The glassy or crystallized powder sample, (particles between 75 and 150 μm) was ultrasonically washed with DIW three times (to remove any small particles adhering to the surface of the larger particles), and with ethanol two times (to dissolved any organic materials), and dried at 90 °C overnight. Exactly 1.5 (± 0.001) g of glassy or crystallized powder was mixed with 15 (± 0.01) ml of DIW in a Teflon vessel that was sealed and held at 90 °C for 7 days. After completion of the PCT, the leachate was filtered and the concentration of ions in the leachate was measured by ICP-ES. The normalized mass release, r_i (g m⁻²) for each element i , was calculated from Eq. (5):

$$r_i = \frac{C_i}{f_i(A/V)}, \quad (5)$$

where C_i (g m⁻³ or ppm) is the concentration of the i element in the leachate; f_i is the mass fraction of element i in the glass; A is the total surface area of the particles (typical value for a sample with $\rho = 2.89$ g cm⁻³ is 1.86×10^{-2} m² g⁻¹) and V is the volume of DIW, (A/V) is

about 1.86×10^3 m⁻¹. The analyzed element concentration, C_i is the average of duplicate samples where the difference was $< \pm 3\%$.

2.6. Other properties

The density of each glass was measured, in duplicate, at room temperature by the Archimedes' method using water as the suspending medium. The average of the two values is given in the Table 3 and the estimated error is $\pm 0.4\%$.

The crystallization behavior for each glass was measured by DTA (DTA-7, Perkin–Elmer Corporation, Norwalk, CT) at a heating rate of 10 °C/min, up to a maximum temperature of 750 °C, in a flowing (20 cm³/min) nitrogen atmosphere. A glass powder sample weighing 40 mg and with a particle size of < 45 μm was used.

The Infrared (IR) spectra of powdered samples pressed in KBr pellets were measured from 400 to 1600 cm⁻¹ (wave number) using a Fourier transform infrared (FT-IR) spectrometer (Perkin–Elmer 1760X). The pellets were prepared by mixing about 5 mg of glassy wasteform with 150 mg of anhydrous KBr. The background for the IR spectra of the glassy samples was corrected for the spectrum of KBr.

3. Results

3.1. Glass formation

The compositions with a waste loading < 55 mass% were easily melted below 1150 °C in 2 h. Since the melts were fluid (estimated viscosity of 5–10 poises), they quickly became homogenous. After casting the melt into a steel mold, it had the appearance of a transparent green glass. Up to 65% waste, no crystalline phases were detected by XRD, indicating that all the Cr₂O₃ in the batch was totally dissolved in the melt.

Since the simulated waste contains SiO₂, Al₂O₃, U₃O₈ and along with other high melting oxides such as ZrO₂ and Cr₂O₃, it was not unexpected that the melting temperature increased with increasing waste loading (see Table 3). Several attempts were made to melt the IP85W and IP90W compositions at 1300 °C, the arbitrarily chosen maximum temperature limit. However, these melts were too viscous to pour from the crucible and totally crystallized during cooling.

Melts cast on a steel plate containing from 70 to 80 mass% waste contained < 1.5 mass% crystalline Cr₂O₃ as identified by XRD. These predominantly glassy samples were black to dark brown in color.

The IP70WSC sample which had been slowly cooled in the electric furnace at 2 °C min⁻¹ from its melting temperature to 300 °C, then cooled slowly to room

temperature, with a hold at 870 °C for 2 h, was primarily glassy with <1.5 mass% of crystalline Cr₂O₃, see XRD pattern in Fig. 1. The XRD pattern for IP70WSC was similar to that for IP70W.

3.2. Solubility of Cr₂O₃

The XRD patterns in Fig. 1 show that the IP65W annealed melt was completely glassy, but a trace amount (<1.5 mass%) of crystalline Cr₂O₃ was detected in the other samples cast on the steel plate. Comparison of the Cr₂O₃ content in the starting batch with the crystalline Cr₂O₃ content in the glasses shows that the solubility limit of Cr₂O₃ in these iron phosphate glass is 2.6 ± 0.1 mass%. The solubility of Cr₂O₃ in AABS glasses is typically <1 mass% [3]. When the starting batch contained more than 2.6 mass% Cr₂O₃ (65 mass% waste loading), crystalline Cr₂O₃ was found in the other iron phosphate melts cast on the steel plate. By using the calibration curve in Fig. 2, the amount of crystalline Cr₂O₃ in the IP70WSC, IP70W, IP75W and IP80W samples was calculated as 1.26, 0.85, 1.18 and 1.30 mass%, respectively.

3.3. Chemical durability

3.3.1. DR

The DR for bulk glassy samples in DIW at 90 °C after 128 days as a function of waste loading is shown in Fig. 4. Generally speaking, the DR decreased with increasing waste loading. When the waste loading was <50 mass%, the DR ranged from 2.2 to 6.6×10^{-7} g cm⁻² min⁻¹.

When the waste loading exceeded 50 mass%, the DR decreased suddenly. The glassy sample containing 65

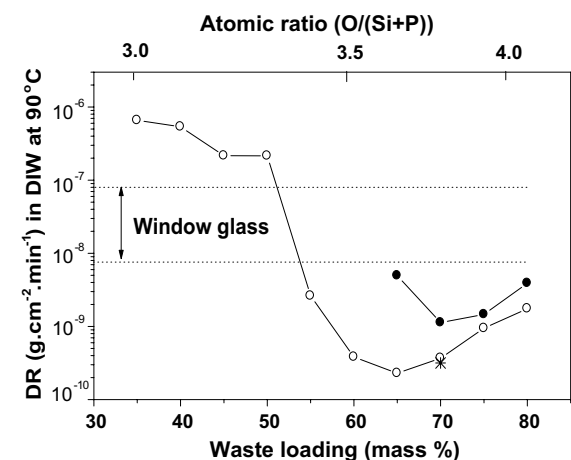


Fig. 4. Dissolution rate (DR) of iron phosphate wasteforms after 128 days in deionized water at 90 °C for glassy (open circles), crystallized at 650 °C for 48 h (solid circles), and sample slowly cooled at 2 °C/min from its melting temperature (star). Estimated error in DR is $\pm 15\%$.

mass% waste had the lowest DR, whereafter, the DR increased slightly with increasing waste loading. All of the samples containing from 55 to 80% waste had a DR which was lower than that of window glass.

Fig. 4 also shows the DR (solid circles) for samples containing ≥ 65 mass% waste, that were deliberately crystallized at 650 °C, see XRD pattern in Fig. 8. The chemical durability of these crystallized samples was still quite good with the DR being essentially the same as that for the glassy samples, except for the sample containing 65 mass% waste, where DR for the crystallized sample was about 10 times higher than for the glass. The DR for all the crystallized samples was also lower than that of window glass.

Except for Cr₂O₃, there were no other detectable XRD peaks in the IP70WSC sample (see Fig. 1), which had been slowly cooled in the furnace. This sample had a glassy appearance and its DR (shown by the star in Fig. 4) was 3.2×10^{-10} g cm⁻² min⁻¹, which is essentially identical to that of the normally annealed sample.

3.3.2. VHT

Fig. 5(a) and (b) show the appearance of the cross-section of the glassy and crystallized IP70W and IP75W samples, respectively, after VHT at 200 °C for 7 days.

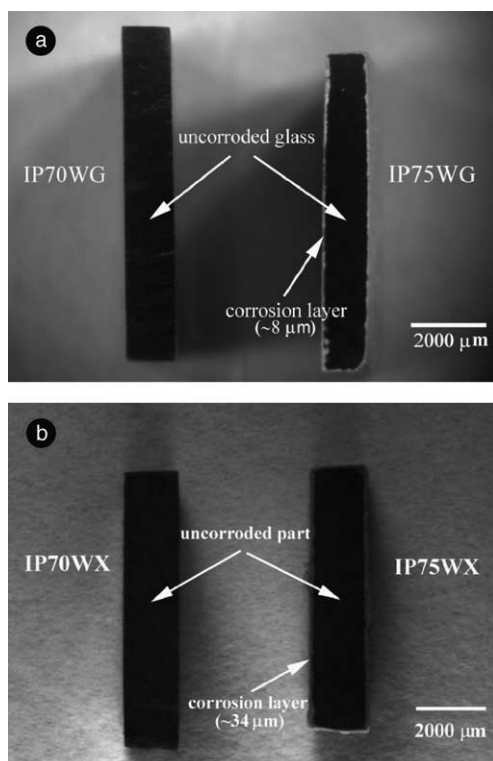


Fig. 5. Appearance of glassy IP70WG and IP75WG (a) and crystallized IP70WX and IP75WX (treated at 650 °C for 48 h) (b) samples after VHT at 200 °C for 7 days.

For the IP70W sample, both glassy and crystallized, there was no visible corrosion layer on the external surface. The pH of the water before and after VHT only changed from 5.5 to 6.2, which indicated very little corrosion had occurred. The weight change of the IP70W sample after VHT (initial weight of 0.39–0.42 g) was barely measurable, being a weight gain of only 0.21–0.46 mg. This small weight gain could be due to hydrated layer or precipitation of corrosion products on the surface. From the sample surface area and test time, the corrosion rate for the glassy and crystallized IP70W sample, was only 0.1–0.2 $\text{g m}^{-2} \text{d}^{-1}$.

After VHT, the pH of the water in contact with the glassy and crystallized IP75W sample was 7.5 and 8.0, respectively compared to the starting pH of 5.5. The thickness of the corroded layer on the glassy and crystallized IP75W sample was only 8 and 34 μm , respectively (see Fig. 5(a) and (b)). Using the change in thickness and the density of the glassy and crystallized IP75W sample of 2.95 and 2.98 g cm^{-3} , respectively, the

amount of sample corroded, m_d , as calculated from Eq. (4) was only 3.3 and 14.5 $\text{g m}^{-2} \text{d}^{-1}$ respectively. These values are much lower than the 140 and 196 $\text{g m}^{-2} \text{d}^{-1}$ that have been reported [9] for LAW-A33 and LD6-5412 borosilicate glasses, respectively.

3.3.3. PCT

The ion concentration in the leachate after completion of PCT, as measured by ICP-ES, and the total mass release for 75–150 μm particles of either glassy or crystallized IP70W and IP75W are given in Tables 4 and 5. After PCT, the pH of the water used for the glassy and crystallized IP70W sample was 9.03 and 9.32, respectively. The pH of the water used for the IP75W sample was 9.51 and 9.58, for the glassy and crystallized sample, respectively.

The normalized element mass release, r_i (g m^{-2}), was calculated from Eq. (5) using the ion concentration in the leachate. The total element mass release was 1.35 and 1.34 g m^{-2} , respectively, for the glassy and

Table 4
Concentration (ppm) of ions found in leachate by ICP-ES after PCT of glassy^a and crystallized^a IP70W and IP75W samples

Element	Concentration (ppm) ^b			
	IP70WG	IP70WX	IP75WG	IP75WX
Al	39.3	31.2	73.5	55.7
Bi	<0.1	0.2	<0.1	0.8
Ca	<0.1	0.1	<0.1	0.2
Cr	0.5	<0.1	0.3	<0.1
Fe	0.3	0.2	0.3	0.7
Na	138	130	184	190
P	73	55.1	90	74
Si	22.5	32.8	30.0	44.2
U	0.2	1.84	0.3	3.27

^a Glassy and crystallized denoted by suffix WG and WX, respectively.

^b Average of duplicate samples, estimated error is $\pm 3\%$.

Table 5
Normalized element mass release (g m^{-2}) from glassy^a and crystallized^a IP70W and IP75W samples after PCT as calculated from ICP-ES data in Table 4

Element	Normalized mass release (g m^{-2}) ^b			
	IP70WG	IP70WX	IP75WG	IP75WX
Al	0.27	0.22	0.48	0.37
Bi	<0.01	<0.01	<0.01	<0.01
Ca	<0.01	<0.01	<0.01	<0.01
Cr	0.01	<0.01	0.01	<0.01
Fe	<0.01	<0.01	<0.01	<0.01
Na	0.55	0.54	0.69	0.73
P	0.27	0.21	0.39	0.32
Si	0.23	0.35	0.29	0.44
U	<0.01	0.02	<0.01	0.03
Total	1.35	1.34	1.88	1.89

^a Glassy and crystallized denoted by suffix WG and WX, respectively.

^b Average of duplicate samples, estimated error is $\pm 3\%$.

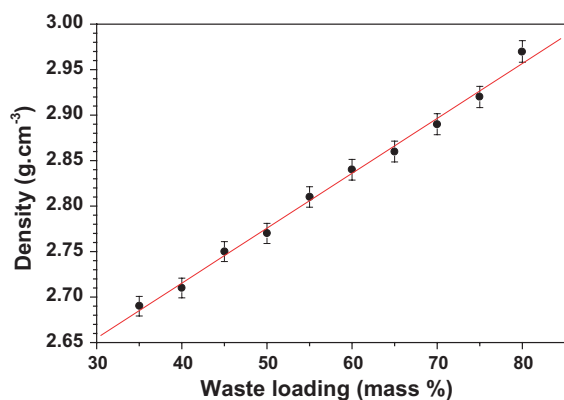


Fig. 6. Density of glassy iron phosphate wasteforms as a function of waste content.

crystallized IP70W sample and was 1.88 and 1.89 g m^{-2} , respectively, for the glassy and crystallized IP75W sample.

As indicated by the ICP-ES analysis of the leachate from the IP70W and IP75W samples, both glassy and crystallized, the elements leached from the samples were primarily Na, P, Al and Si. The amount of Ca, Fe, Cr, U and Bi elements leached from these samples was very small (<1 ppm). This is noticed that the solubility of former oxides is higher than that of the latter. It may imply that the oxides of Ca, Fe, Cr, V and Bi in the phosphate wasteforms are stable, whether in glassy or crystallization form.

3.4. Density

Fig. 6 shows an increase in density with waste loadings. The density is not a particularly sensitive structural

property and depends primarily upon composition. Because of the heavy oxides in the waste, such as U_3O_8 , Bi_2O_3 and Cr_2O_3 , an increase in density with waste loading is expected. A higher density is advantageous to waste vitrification, since the volume of vitrified waste is reduced for any given waste loading.

4. Discussion

4.1. Glass forming ability

In the present study, all of the compositions containing up to 80 mass% of simulated waste could be melted between 1100 and 1300 °C in 2 h and when cast on the steel plate were either totally or predominantly glassy. Even the IP70WSC melt, which was cooled slowly at 2 °C min^{-1} in the melting furnace, did not crystallize during cooling as confirmed by XRD. These facts indicate that the compositions containing $\leq 70\%$ waste are good glass formers and the tendency for crystallization is low.

The DTA curves for the glassy samples showed no prominent peaks due to crystallization when the sample was heated to 750 °C (where these samples stuck to the DTA crucible) or up to its melting temperature. This implied that these glassy samples had good thermal stability and glass forming ability.

The good glass forming ability of these glasses can be explained by the cross-linking density of the network structure. When the atomic ratio of O/P = 3, the $(\text{PO}_4)^{3-}$ tetrahedra are joined through P–O–P bonds to form long chains, that promote glass formation. With increasing waste loading, the P_2O_5 content decreases as the concentration of other metal oxides increases. The P–O–P bonds are broken with increasing O/P ratio, such

Table 6

Batch composition, in atomic percent, of high chrome iron phosphate wasteforms

Wasteform ID	IP35W	IP40W	IP45W	IP50W	IP55W	IP60W	IP65W	IP70W	IP75W	IP80W
O	65.61	64.72	63.81	62.88	61.94	60.98	60.00	59.00	57.98	56.94
Al	3.11	3.59	4.07	4.57	5.07	5.59	6.11	6.65	7.19	7.75
Bi	0.10	0.11	0.13	0.14	0.16	0.17	0.19	0.21	0.22	0.24
Ca	0.29	0.33	0.38	0.43	0.47	0.52	0.57	0.62	0.67	0.72
Cr	0.40	0.46	0.52	0.58	0.65	0.71	0.78	0.85	0.92	0.99
Fe	0.85	0.98	1.11	1.25	1.39	1.53	1.67	1.82	1.97	2.12
La	0.03	0.04	0.04	0.05	0.05	0.06	0.06	0.07	0.07	0.08
Na	6.34	7.13	8.30	9.30	10.33	11.38	12.45	13.54	14.64	15.78
P	20.29	19.02	17.73	16.41	15.06	13.70	12.3	10.88	9.43	7.95
Si	2.01	2.32	2.63	2.95	3.28	3.61	3.95	4.30	4.65	5.01
U	0.24	0.28	0.32	0.36	0.39	0.43	0.48	0.52	0.56	0.60
Zr	0.18	0.21	0.24	0.27	0.30	0.33	0.36	0.39	0.42	0.46
O/(Si + P) ^a	2.94	3.03	3.13	3.25	3.38	3.52	3.69	3.89	4.07	4.39

^a O/(Si + P): the atom ratio of oxygen (O) to phosphorus (P) plus silicon (Si) silicon is assumed to bond to oxygen in the same way as phosphorus.

that $(\text{P}_2\text{O}_7)^{4-}$ groups are formed at $\text{O}/\text{P} = 3.5$, and only isolated $(\text{PO}_4)^{3-}$ tetrahedra are present at $\text{O}/\text{P} = 4$.

In the present study, both SiO_2 and P_2O_5 were the glass network former and the ratio of $\text{O}/(\text{Si} + \text{P})$ varied from 2.94 to 4.39 (see Table 6) with increasing waste loading. Although the chains of $(\text{PO}_4)^{3-}$ tetrahedra became shorter, the other metal ions, such as Fe^{3+} , Cr^{3+} , Al^{3+} and Zr^{4+} ions could connect these isolated $(\text{PO}_4)^{3-}$ tetrahedra, thereby increasing the cross-linking density of the network structure. If these former cations act as a type of cross linking agent, the concentration of glass former ions would not significantly decrease with increasing waste loading, and the glass forming ability may not decrease with increasing waste loading. Samples with high cross-linking density were resistant to crystallization. This is the reason that the glassy samples were difficult to crystallize and no prominent crystallization peak occurred in the DTA curve.

4.2. Cr_2O_3 solubility

Since the source of Cr_2O_3 in the present study was from Na_2CrO_4 , which has a melting point of 792 °C, it is assumed that the chrome oxide was dissolved in the melt during melting at 1250 °C. In a similar study, Li [10] reported that no segregated chrome was observed on the melt surface at a melting temperature of 1300 °C. The source of Cr_2O_3 in Li's study, was Cr_2O_3 (some precipitated as $\text{Cr}_2\text{O}_3 \cdot x\text{H}_2\text{O}$). In our case, the chrome oxide from Na_2CrO_4 is expected to be totally dissolved in the melt during melting.

The solubility of Cr_2O_3 would likely decrease with decreasing temperature, such that the melt would become saturated with Cr_2O_3 that could crystallize or precipitate from the melt during cooling. Although crystalline Cr_2O_3 was present in annealed melts containing ≥ 70 mass% waste, the solubility limit for Cr_2O_3 in the glass was up to 2.6%, according to the results in Fig. 3.

4.3. Chemical durability

When the waste loading exceeded 50 mass%, the DR was lower than that of window glass (see Fig. 4). The exact reason why the DR of glasses containing <50 mass% waste was higher is not known, but could be explained by the O/P atomic ratio. According to earlier work [4], iron phosphate glasses tend to have their best chemical durability when the O/P ratio is between 3.4 and 3.8. It will be recalled that an O/P ratio of 3, 3.5 and 4 corresponds to metaphosphate, $(\text{PO}_3)^{1-}$ chains, isolated pyrophosphate $(\text{P}_2\text{O}_7)^{4-}$ groups and isolated orthophosphate $(\text{PO}_4)^{3-}$ groups, respectively. For the compositions in Table 6, where the waste loading was <50 mass%, the $\text{O}/(\text{Si} + \text{P})$ ratio varied from 2.94 to 3.25 which is close to the metaphosphate composition. Be-

cause of the large number of $\text{P}-\text{O}-\text{P}$ bonds, which are easy to hydrate, in these glasses, their chemical durability is reduced.

During the chemical durability measurement, it is likely that some small fraction of the alkaline and alkaline earth cations are exchanged by H_3O^+ ions and are released to the leachate. These cations would increase the pH of the solution.

With increasing waste loading, the $\text{O}/(\text{Si} + \text{P})$ ratio increases and the number of $\text{P}-\text{O}-\text{P}$ bonds is reduced as the chains of $(\text{PO}_3)^{1-}$ tetrahedra are broken, and more $(\text{P}_2\text{O}_7)^{4-}$ groups form in the structure. The reduction of $\text{P}-\text{O}-\text{P}$ bonds leads to an increase in the chemical durability as the waste loading increases. Furthermore, Me (Me^{3+} or Me^{4+})- $\text{O}-\text{P}$ bonds replace the $\text{P}-\text{O}-\text{P}$ bonds with increasing waste loading. Since the intermediate cations, such as Al^{3+} , Fe^{3+} , Cr^{3+} and Zr^{4+} can stabilize the bridging $\text{Me}-\text{O}-\text{P}$ bonds [11], these strong bonds are difficult to hydrolyze. On the other hand, the replacement of $\text{P}-\text{O}-\text{P}$ bonds would increase the cross linking effect of multivalent ions, which blocks water diffusion to a limiting step of phosphate glass dissolution [12]. Therefore, the chemical durability improves with increasing waste loading. The small number of easily hydrated $\text{P}-\text{O}-\text{P}$ bonds, the low water diffusion in the network and the strong $\text{Me}-\text{O}-\text{P}$ bonds in these phosphate glasses are a general explanation for why the best chemical durability (lowest DR) occurred at a waste loading of 60–70 mass% where the $\text{O}/(\text{Si} + \text{P})$ was 3.5–3.8.

The structural changes that occur with increasing waste loading can be seen in the IR spectra in Fig. 7. The absorption located at 1243–1285 cm^{-1} , assigned to the anti-symmetric stretching vibration of $\text{P}-\text{O}-\text{P}$ bonds in

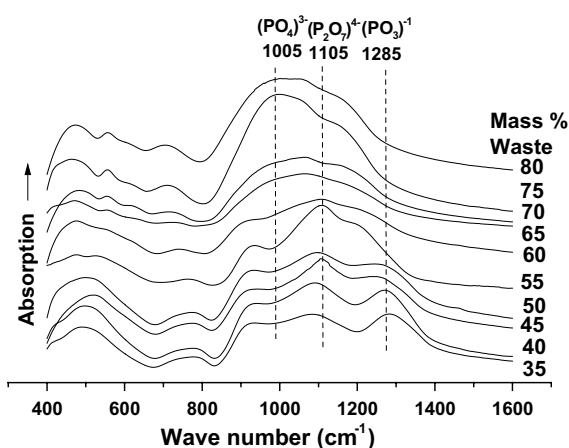


Fig. 7. Infrared spectra of iron phosphate wasteforms containing the percent waste shown for each curve. The bands at 1285, 1105 and 1005 cm^{-1} are assigned as the anti-symmetric stretching vibration of $\text{O}-\text{P}$ bonds in $(\text{PO}_3)^{1-}$, $(\text{P}_2\text{O}_7)^{4-}$ and $(\text{PO}_4)^{3-}$ groups, respectively.

the terminal groups in $(\text{PO}_3)^{1-}$ chains [13], decreases with increasing waste content. When the waste content reached 55 mass%, this peak had essentially disappeared. This change indicates that the $(\text{PO}_3)^{1-}$ chains in the structure were gradually replaced by $(\text{P}_2\text{O}_7)^{4-}$ groups, which produced the absorption at 1105 cm^{-1} that has been assigned [14] to anti-symmetric stretching vibrations of P–O–P bonds in the $(\text{P}_2\text{O}_7)^{4-}$ groups. The absorption at 1105 cm^{-1} becomes increasingly prominent up to a waste content of 55 mass%. The chemical durability is improved as $(\text{P}_2\text{O}_7)^{4-}$ groups are formed, because of the decreasing number of easily hydrated P–O–P bonds. When the waste content exceeds 55 mass%, the $(\text{P}_2\text{O}_7)^{4-}$ groups should dominate the glass structure.

With increasing waste loading, isolated $(\text{PO}_4)^{3-}$ groups in the glass structure gradually increase as indicated by the increasing absorption at 1005 cm^{-1} . Thus, the network structure contains an increasing number of unoccupied sites, which the metal cations can occupy. This is the reason that iron phosphate glass can accommodate cations of different size and charge. Due to the stability of O–Me–O–P bonds [11], the Me cations, which are accommodated in the phosphate glass improves the chemical durability of iron phosphate glasses. In the present study, the PCT data (Table 4) show that the metal cations are tightly bonded, since <1 ppm of metal ions, such as Fe^{3+} , Cr^{3+} , Bi^{3+} , U^{3+} and Zr^{4+} ions were leached from the sample. These O–Me–O–P bonds firmly bond these metal cations within the glass network structure.

The high solubility limit of Cr_2O_3 in the iron phosphate glass should improve its chemical durability, since Cr^{3+} ions might connect isolated $(\text{PO}_4)^{3-}$ tetrahedra just as the Fe^{3+} and Fe^{2+} ions connect the $(\text{P}_2\text{O}_7)^{4-}$ groups in iron phosphate glasses [6]. Thus Cr_2O_3 could increase the degree of cross-linking in the network of the present waste glasses.

It should be mentioned that the presence of small amounts of crystalline Cr_2O_3 in the samples containing ≥ 70 mass% waste did not adversely affect the chemical durability. Crystalline Cr_2O_3 is stable in DIW at $90\text{ }^\circ\text{C}$.

The XRD pattern in Fig. 8 for the IP70W sample crystallized at $650\text{ }^\circ\text{C}$ for 48 h is typical for all four deliberately crystallized samples, which contained from 65 to 80 mass% waste. The same crystalline phases, $\text{Na}_3\text{Cr}_2\text{P}_3\text{O}_{12}$ (JCPDS Card #84-1203) and $\text{NaFe}_3\text{P}_3\text{O}_{12}$ (45-0126) were found in each crystallized sample. Small amounts of possibly UO_3 (84-1203) and FePO_4 (33-0666) were also present, although their identification is less certain. On the basis of the XRD pattern, several components, such as SiO_2 , Al_2O_3 , ZrO_2 along with a part of the P_2O_5 are believed to have remained in a residual glassy phase in each sample.

The chemical durability of the crystallized samples was still quite good with the DR being essentially the same as for the glassy samples (see Fig. 4), except for the

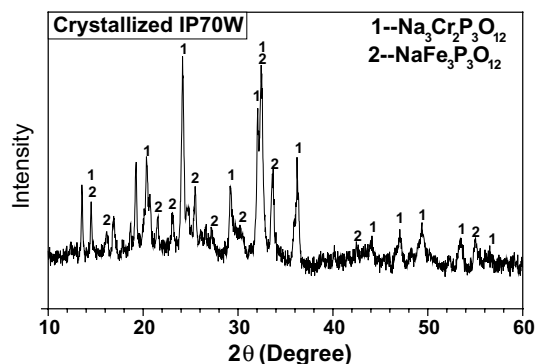


Fig. 8. Powder XRD pattern of iron phosphate wasteform containing 70 mass% waste after 48 h heat treatment at $650\text{ }^\circ\text{C}$.

sample containing 65 mass% waste, where the DR for the crystallized sample was slightly higher. These crystalline phases apparently have a good corrosion resistance to DIW at 90, since they contain stable Fe–O–P–O–Fe or Cr–O–P–O–Cr bonds [15]. It should be noted that the residual glass phase is chemically durable, since a large fraction of Na^+ and P^{5+} ions were in the $\text{Na}_3\text{Cr}_2\text{P}_3\text{O}_{12}$ and $\text{NaFe}_3\text{P}_3\text{O}_{12}$ crystal phases. The number of easily hydrated P–O–P bonds is expected to be low in these deliberately crystallized iron phosphate samples, as evidenced by their high chemical durability.

5. Conclusion

The HLW at Hanford WA, containing up to 4.5 mass% chrome oxide can be vitrified into chemically durable wasteforms by simply adding 25–35 mass% phosphate and melting the mixture at $1150\text{--}1250\text{ }^\circ\text{C}$ for a few hours.

These glasses had an exceptionally good chemical durability at waste loadings ranging from 60 to 75 mass%. The total elemental mass release determined by PCT (ASTM C-1285-97) for either glassy or deliberately crystallized wasteforms that contained 70 or 75 mass% waste loading was less than 1.5 and 2.0 g m^{-2} , respectively. Similarly, the corrosion rate of these two glasses was <0.2 and $3.5\text{ g m}^{-2}\text{ d}^{-1}$, respectively, as determined by VHT at $200\text{ }^\circ\text{C}$ for 7 days.

Crystallization is often assumed to reduce the chemical durability, but that was not the case in the present study. When the glassy wasteforms were deliberately crystallized at $650\text{ }^\circ\text{C}$ for 48 h, the corrosion rate remained unchanged for the wasteform containing 70 mass% waste and increased only slightly to $14.4\text{ g m}^{-2}\text{ d}^{-1}$ for the crystallized wasteform containing 75 mass% waste.

The atomic ratio of O/(Si+P) at these high waste loadings, as calculated from the batch composition, was between 3.7 and 4.1. Therefore, the concentration of easily hydrated P–O–P bonds in the wasteforms should

be small which is consistent with their excellent chemical durability.

The intermediate metal cations, such as Al^{3+} , Fe^{3+} , Cr^{3+} , and Zr^{4+} , are believed to form O–Me–O–P bonds in these glasses that connect isolated $(\text{P}_2\text{O}_7)^{4-}$ or $(\text{PO}_4)^{3-}$ groups at high waste loadings so as to provide a high resistance to crystallization. Although trace amounts of crystalline Cr_2O_3 were present in wasteforms containing ≥ 70 mass% waste, no crystallization peaks were observed when the glasses containing 70 or 75 mass% waste were reheated to 750 °C during DTA. Similarly, no significant crystallization was detectable by XRD when a melt containing 70 mass% waste was cooled at 2 °C min^{-1} in the melting furnace to room temperature with a 2 h hold at 870 °C.

The outstanding chemical durability, high waste loading, good glass forming characteristics and reasonable melting temperature (≤ 1250 °C) and time (< 6 h) suggest that simply adding 25–35 mass% phosphate to the high chrome wastes stored at Hanford should be a technically feasible and cost effective way of vitrifying these wastes.

Acknowledgements

Work supported by Department of Energy (DOE) under EMSP grant DOE DE-FG07-96ER45618.

References

- [1] J.M. Perez, Jr., D.K. Peler, D.F. Bickford, D.M. Strachan, D.E. Day, M.B. Triplett et al., High-Level Waste Melter Study Report, PNNL-13582, July 2001.
- [2] R.A. Kirkbride, Tank farm contactor operation and utilization plan (TWRS-OUT), HNF-SD-WM-SP-012, Rev. 2, CH2M Hill Hanford Group, Richland Washington, 2000.
- [3] X. Feng, P.R. Hrma, J.H. Westsik, Jr., N.R. Brown, M.T. Schweiger, H. Li, et al., Glass Optimization for Vitrification of Hanford site Low-Level Tank Waste, PNNL-10918, Pacific Northwest Laboratory, Richland, WA, 1996.
- [4] D.E. Day, Z. Wu, C.S. Ray, P.R. Hrma, J. Non-Cryst. Solids 241 (1998) 1.
- [5] M. Karabulut, G.K. Marasinghe, C.S. Ray, D.E. Day, O. Ozturk, G.D. Waddill, J. Non-Cryst. Solids 249 (2–3) (1999) 106.
- [6] X. Yu, D.E. Day, J. Non-Cryst. Solids 215 (1997) 21.
- [7] PNNL Technical Document, Vapor Phase Hydration Test Procedure, GDL-VHT, Rev. 1, Pacific Northwest National Laboratory, Richland, WA, 2000.
- [8] ASTM Standard Test Method for Determining Chemical Durability of Nuclear, Hazardous, and Mixed Waste Glasses: The Product Consistency Test, C 1285-97.
- [9] A. Jiricka, J.D. Vienna, P. Hrma, D.M. Strachan, J. Non-Cryst. Solids 292 (2001) 25.
- [10] H. Li, P. Hrma, M.H. Langowski, J. Hlavac, in: V. Jain, D. Peeler (Eds.), Ceramic Transaction, vol. 72, The American Ceramic Society, Westerville, OH, 1996, p. 299.
- [11] U. Hoppe, G. Walter, R. Kranold, D. Stachel, J. Non-Cryst. Solids 263&264 (2000) 29.
- [12] M.G. Mesko, D.E. Day, B.C. Bunker, Waste Management 20 (4) (2000) 271.
- [13] A.M. Efimov, J. Non-Cryst. Solids 209 (1997) 209.
- [14] B. Karmakar, P. Kundu, R.N. Dwivedi, J. Non-Cryst. Solids 289 (2001) 155.
- [15] N. Fanjat, G. Lucazeau, A.J. Dianoux, J. Phys. Chem. Solids 53 (3) (1992) 395.